

Analysis of an Eddy Current Sensor for Liquid Pressure Measuring by FEM simulation

Xu Linsen, Luo Minzhou
Institute of Intelligent Machines,
Chinese Academy of Sciences
Hefei, China
Xls008@tom.com

Xu Linsen, Luo Minzhou, Han Feng, Hu Xiaojuan
Changzhou Institute of Mechatronics Engineering,
Changzhou, China

Abstract—The influence of the uniform pressure on the induced magnetic field and the eddy distribution is shown in this paper to provide foundation for the design of an eddy current sensor for measuring the liquid pressure. For reviewing the distribution characters of the magnetic field and the eddy current, the basic principle of the eddy current sensor for liquid pressure measuring is discussed firstly, and the mechanical analysis to the diaphragm of the sensor is carried out to describe its deformation under the pressure, which influences the magnetic flux density of the system. Then the finite element method (FEM) model is built using the electromagnetic theory and the functional analysis to get the magnetic flux density and the current density of the coil. At last, the simulation results is got, which shows the change of the magnetic flux density when the pressure being loaded.

Keywords—eddy current sensor pressure measuring finite element method

I. INTRODUCTION

A linear sensor for liquid pressure measuring is a key part for monitoring and controlling an air-condition system, whose precision have important influence on the comfortable quality, the intelligent quality and the energy saving quality of the air-condition system.

At present, most sensors for liquid pressure measuring are based on piezo-resistance or capacitance. The dynamic error of the piezoresistive sensor is big, and its stability and reliability are poor, which is falling into use step by step. The ceramic capacity sensor has good dynamic performance, stability and reliability, but which is expensive. The eddy current sensor is a novel use of electromagnetics for liquid measuring, which has the same measuring capability as the ceramic capability sensor, but its cost-effective is higher.

At the present time, the study about the influence of the coil parameters on the sensor performance is mostly to change the coil geometrical parameters and calculate by the corresponding theories^[1], or to model and simulate from the basic theories^[2-3], whose modeling tests are complex. The above methods both increase the difficulty of designing the eddy current sensor for liquid pressure measuring.

The finite element method (FEM) is widely used in electromagnetics lately, and its modeling and simulating fit the

engineering need. The electromagnetic fields distribution of the linear eddy current sensor is discussed in this paper by FEM simulation.

II. BASIC PRINCIPLE OF EDDY CURRENT SENSOR FOR MEASURING LIQUID PRESSURE

The principle diagram of the eddy current sensor is shown as Fig.1. When a metal diaphragm has been set in the alternating magnetic field ϕ_1 produced by a coil with high frequency current i_1 , a closed current loop i_2 comes into being in it as a result of electromagnetic induction function, which is called “eddy current loop”. Then a magnetic field ϕ_2 comes into being to counteract the change of the former alternating magnetic field ϕ_1 . Fig 1(a) shows the condition when the diaphragm is subjected to zero pressure, and Fig 1(b) shows the condition when the diaphragm is subjected to a uniform pressure p . The uniform pressure deforms the diaphragm and causes the biggest displacement in its center. The current loop i_2 is related to the distance Δz between the coil and the diaphragm, which means the magnetic field ϕ_2 is also changed with it. So the impedance, the inductance and the quality factor are related to the distance Δz , and which can be outputted as electric quantity parameters.

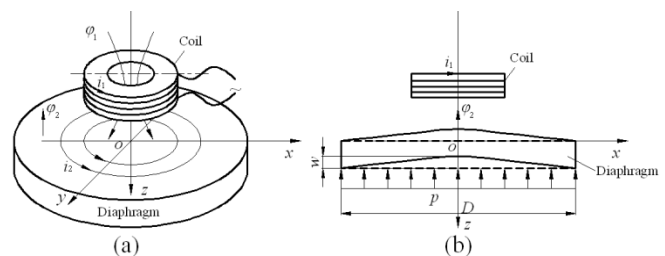


Figure 1 Principle Diagram of Eddy Current Sensor for cool-medium pressure measuring

This paper discusses the influence of the uniform pressure on the induced magnetic field and the eddy distribution by finite element method.

III. DEFORMATION OF DIAPHRAGM

Fig 1(b) shows the deformation of the diaphragm when it subjects to a uniform pressure. It is advantageous that the

bending formulas of the circular sheet are built in the polar coordinates. And the deflection w and the load p is the functions of the polar coordinates r and θ , namely $w=w(r, \theta)$, $p=p(r, \theta)$. The following equation can be got according to the relationship between polar coordinates and Cartesian coordinates.

$$\begin{cases} \frac{\partial w}{\partial x} = \cos\theta \frac{\partial w}{\partial r} - \frac{\sin\theta}{r} \frac{\partial w}{\partial \theta} \\ \frac{\partial w}{\partial y} = \sin\theta \frac{\partial w}{\partial r} + \frac{\cos\theta}{r} \frac{\partial w}{\partial \theta} \end{cases} \quad (1)$$

The following functions are got by repeating the above calculation

$$\begin{cases} \frac{\partial^2 w}{\partial x^2} = \cos^2\theta \frac{\partial^2 w}{\partial r^2} - \frac{2\sin\theta\cos\theta}{r} \frac{\partial^2 w}{\partial r \partial \theta} + \frac{\sin^2\theta}{r} \frac{\partial w}{\partial r} \\ \quad + \frac{2\sin\theta\cos\theta}{r^2} \frac{\partial w}{\partial \theta} + \frac{\sin^2\theta}{r^2} \frac{\partial^2 w}{\partial \theta^2} \\ \frac{\partial^2 w}{\partial y^2} = \sin^2\theta \frac{\partial^2 w}{\partial r^2} + \frac{2\sin\theta\cos\theta}{r} \frac{\partial^2 w}{\partial r \partial \theta} + \frac{\cos^2\theta}{r} \frac{\partial w}{\partial r} \\ \quad - \frac{2\sin\theta\cos\theta}{r^2} \frac{\partial w}{\partial \theta} + \frac{\cos^2\theta}{r^2} \frac{\partial^2 w}{\partial \theta^2} \\ \frac{\partial^2 w}{\partial x \partial y} = \sin\theta\cos\theta \frac{\partial^2 w}{\partial r^2} + \frac{\cos^2\theta - \sin^2\theta}{r} \frac{\partial^2 w}{\partial r \partial \theta} - \frac{\sin\theta\cos\theta}{r} \frac{\partial w}{\partial r} \\ \quad - \frac{\cos^2\theta - \sin^2\theta}{r^2} \frac{\partial w}{\partial \theta} - \frac{\sin\theta\cos\theta}{r^2} \frac{\partial^2 w}{\partial \theta^2} \end{cases} \quad (2)$$

From the above equation, we can get

$$\nabla^2 w = \frac{\partial^2 w}{\partial r^2} + \frac{1}{r} \frac{\partial w}{\partial r} + \frac{1}{r^2} \frac{\partial^2 w}{\partial \theta^2}. \quad (3)$$

So the differential equation of the elastic surface can be written as

$$R \left(\frac{\partial^2}{\partial r^2} + \frac{1}{r} \frac{\partial}{\partial r} + \frac{1}{r^2} \frac{\partial^2}{\partial \theta^2} \right) \left(\frac{\partial^2 w}{\partial r^2} + \frac{1}{r} \frac{\partial w}{\partial r} + \frac{1}{r^2} \frac{\partial^2 w}{\partial \theta^2} \right) = p. \quad (4)$$

The boundary conditions of the sensor for cool-medium pressure measuring are:

- (1) The force on the diaphragm is a uniform pressure p .
- (2) There is no hole in the center of the diaphragm.

The around side of the diaphragm is fixed, that is,

$$(w)_{r=\frac{D}{2}} = 0, \left(\frac{dw}{dr} \right)_{r=\frac{D}{2}} = 0.$$

So the deformation equation of the diaphragm is known as

$$w = \frac{pD^4}{1024R} \left(1 - \frac{4r^2}{D^2} \right)^2. \quad (5)$$

The above equation is the deformation of the diaphragm subjected to a uniform pressure p . The deformation causes the center part of the diaphragm moving to the coil, which has an influence on the alternating magnetic field φ_1 .

IV. EDDY CURRENT SENSOR MODEL OF FEM SIMULATION

The magnetic fields shown in Fig (1) are three-dimension, and it is possible to build a three-dimension eddy current field model to solve. But they can be simplified as the axis-symmetric quasi-static alternating electromagnetic fields considering the magnetic fields in the eddy current sensor being quasi-static alternating fields. If the magnetic field is

axis-symmetric and its distribution in some axis-symmetrical section has been got, its distribution in the whole area to be analyzed is known. The symmetric section is a plane, which makes calculating much easier. The FEM model of the quasi-static alternating electromagnetic field of the eddy current sensor is built to simulate the induced magnetic field and the eddy distribution in this paper.

Based on the solved model shown in Fig 1, the Maxwell equations can be transformed as follows,

$$\begin{cases} \nabla \times \mathbf{H} = \mathbf{J} \\ \nabla \times \mathbf{E} = -j\omega \mathbf{B} \\ \nabla \cdot \mathbf{B} = 0 \\ \nabla \cdot \mathbf{D} = 0 \end{cases} \quad (6)$$

In the equation \mathbf{B} represents the magnetic flux density, \mathbf{H} represents the magnetic field intensity, \mathbf{E} represents the electric field intensity, \mathbf{J} represents the coil current density, \mathbf{D} represents the displacement density and ω represents the excitation angular frequency.

The constitutive relation in the magnetic field is

$$\mathbf{B} = \mu \mathbf{H}, \quad \mathbf{J} = \sigma \mathbf{E}, \quad (7)$$

where μ represents the medium magnetic permeability, and σ represents the medium electric conductivity.

The magnetic fields shown in Fig (1) are axis-symmetric about z axis, and the coil is induced by sine alternating current, which fit in with the definition of axis-symmetric transverse harmonic field^[4], so the model has the characters as follows

(1) All field quantity and the electromagnetic potential function have nothing to do with the circumferential coordinates.

(2) According to Lorenz gauge, the magnetic vector potential \mathbf{A} only has relationship with the circumferential coordinates, namely $\mathbf{A} = \mathbf{A}_\theta \mathbf{e}_\theta$, and its divergence $\nabla \cdot \mathbf{A} = 0$.

(3) The electric field intensity only has the circumferential component.

The circumferential component of the magnetic flux density and the electric field intensity are zero, that is,

$$\frac{H_\theta}{\mu} = \mathbf{B}_\theta = \frac{\partial A_\theta}{\partial \theta} = 0.$$

In a word, the governing equation of the coil current density \mathbf{J} and the magnetic vector potential \mathbf{A} is shown as

$$\begin{cases} \Omega: \frac{\partial^2 \mathbf{A}}{\partial z^2} + \frac{\partial}{\partial r} \left[\frac{1}{r} \frac{\partial(r\mathbf{A})}{\partial r} \right] = -\mu \mathbf{J} + j\omega \sigma \mu \mathbf{A} \\ \quad \mathbf{s}_1: \mathbf{A} = \mathbf{A}_0 \\ \quad \mathbf{s}_2: \frac{1}{r} \frac{\partial(r\mathbf{A})}{\partial n} = -\mu \mathbf{H} \end{cases} \quad (8)$$

In the equation \mathbf{A} and \mathbf{J} are scalar quantities. And \mathbf{s}_1 and \mathbf{s}_2 represent respectively the first boundary conditions and the second boundary conditions. Suppose $\mu' = \mu/r$, $\sigma' = \sigma/r$, then the above equations can be written as

$$\begin{cases} \Omega: \frac{\partial}{\partial z} \left(\frac{1}{\mu'} \frac{\partial(r\mathbf{A})}{\partial z} \right) + \frac{\partial}{\partial r} \left[\frac{1}{r} \frac{\partial(r\mathbf{A})}{\partial r} \right] = -\mathbf{J} + j\omega \sigma'(r\mathbf{A}) \\ \quad \mathbf{s}_1: r\mathbf{A} = r\mathbf{A}_0 \\ \quad \mathbf{s}_2: \frac{1}{r} \frac{\partial(r\mathbf{A})}{\partial n} = -\mu' \mathbf{H} \end{cases} \quad (9)$$

Its energy functional W is

$$W(u) = \iint_{\Omega} \frac{\beta}{2r} \left[\left(\frac{\partial u}{\partial z} \right)^2 + \left(\frac{\partial u}{\partial r} \right)^2 \right] dzdr - \iint_{\Omega} J u dzdr + \iint_{\Omega} \frac{1}{2r} j \omega \sigma u^2 dzdr + \iint_{s_2} H u dzdr. \quad (10)$$

And the conditional variational problem equals to (9) is

$$W(u) = \iint_{\Omega} \left\{ \frac{\beta}{2r} \left[\left(\frac{\partial u}{\partial z} \right)^2 + \left(\frac{\partial u}{\partial r} \right)^2 \right] - J u + \frac{1}{2r} j \omega \sigma u^2 \right\} dzdr + \iint_{s_2} H u dzdr = \min, \quad (11)$$

where the boundary conditions are $s_1: u = u_0$.

Regarding the triangular elements e , the linear interpolation function of its magnetic vector potential u is as follows

$$u = \sum_{h=i,j,m} N_h u_h, \quad (12)$$

where N_h is the shape function, that is

$$N_k = \frac{1}{2\Delta} (a_h + b_h z + c_h r) u_h, \quad (h=i, j, m). \quad (13)$$

Here a_h, b_h, c_h ($h=i, j, m$) are all constants determined by the nodes location, and Δ is the area of the triangular elements. The first partial derivative of Equation (12) to z and r are respectively

$$\begin{cases} \frac{\partial u}{\partial z} = \frac{1}{2\Delta} (b_i u_i + b_j u_j + b_m u_m) \\ \frac{\partial u}{\partial r} = \frac{1}{2\Delta} (c_i u_i + c_j u_j + c_m u_m) \end{cases}. \quad (14)$$

And the energy functional of the element e is

$$W_e(u) = \iint_{\Delta} \left\{ \frac{\beta}{2r} \left[\left(\frac{\partial u}{\partial z} \right)^2 + \left(\frac{\partial u}{\partial r} \right)^2 \right] - J u \right\} dzdr + \iint_{\Delta} \frac{1}{2r} j \omega \sigma u^2 dzdr. \quad (15)$$

The first partial derivatives of the above equation to the magnetic potential u_l ($l=i, j, m$) of every node are got as follows

$$\frac{\partial W_e}{\partial u_l} = \sum_{h=i,j,m} k_{lh} u_h - p_l, \quad (l=i, j, m), \quad (17)$$

here

$$p_l = \iint_{\Delta} J N_l dzdr = \frac{J \Delta}{3}, \quad (l=i, j, m), \quad (18)$$

$$k_{lh} = \frac{\beta}{4\Delta r^*} (b_l b_h + c_l c_h), \quad (19)$$

$$r^* = 1.5 / \left(\frac{1}{r_i + r_j} + \frac{1}{r_j + r_m} + \frac{1}{r_m + r_i} \right). \quad (20)$$

And

$$\frac{\partial W_e''}{\partial u_l} = \iint_{\Delta} j \omega \sigma \frac{\sum_{h=i,j,m} N_h u_h}{\sum_{h=i,j,m} N_h r_h} N_l dzdr, \quad (l=i, j, m). \quad (21)$$

After the values rA (u) of all nodes being calculated by FEM, the magnetic flux density and the coil current density can be got as follows

$$B = B_z l_z + B_r l_r = \frac{1}{2\Delta r} (c_i u_i + c_j u_j + c_m u_m) l_z - \frac{1}{2\Delta r} (b_i u_i + b_j u_j + b_m u_m) l_r. \quad (22)$$

And

$$J_e = \frac{\sqrt{2}}{2} \iint_{\Delta} (-j \omega \sigma A) dzdr = -\frac{\sqrt{2}}{6} j \omega \sigma \left(\frac{u_j + u_m}{r_j + r_m} + \frac{u_m + u_i}{r_m + r_i} + \frac{u_i + u_j}{r_i + r_j} \right). \quad (23)$$

The values of the magnetic vector potential should not be A , but rA when constructing the magnetic figure, since the rA counter represents the magnetic figure.

V. SIMULATION ANALYSIS

It is known from the measuring demands that the characters of the parts, which are as follows. The external diameter of the coil $D_1=7\text{mm}$, and its inner diameter of the coil $d_1=1\text{mm}$. Its turn number of the coil $n=500$, and the exciting voltage $V=5\cos 3000t$. The diaphragm diameter $D=14\text{mm}$, and its thickness $s=0.39\text{mm}$. The above data is the base of our simulation analysis. Because the first boundary conditions of the conditional variational problem must be brought forward as the constraint conditions, they are called as the imposing boundary conditions. The second boundary conditions are the boundaries between the media, which are called as the natural boundary conditions and are automatically satisfied by calculating the functional for the extremum. So we only need consider the first boundary conditions. For the above model of the axis-symmetric quasi-static alternating magnetic, it is feasible to analyze a symmetric section instead of the whole area, which is shown as Fig.2. And the first boundary conditions are the sides of the plane area shown in Fig.2, so the peripheral magnetic potential is supposed to be zero according to the conditions of the eddy current sensor.

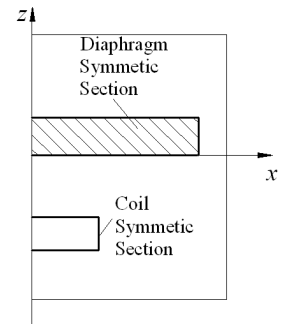


Fig 2 Boundary Conditions of Axis-symmetric Quasi-static Alternating Magnetic Field

Fig.3 shows the magnetic flux density before the uniform pressure being loaded on the diaphragm. And the magnetic flux

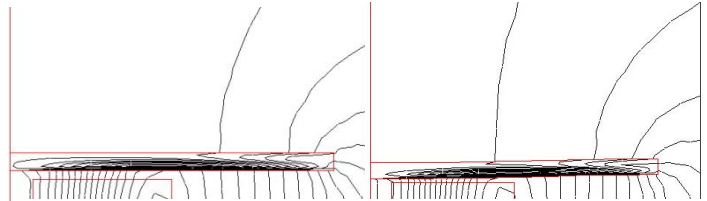


Fig.3 Magnetic Flux Density Before Pressure Being Loaded.

Fig.4 Magnetic Flux Density When Pressure Being Loaded

density when the pressure being loading in the same conditions is shown as Fig 4. It can be known that the magnetic flux density when the pressure being loaded is smaller than it before the pressure being loaded. And the coil current is smaller after the diaphragm deforming, whose value is 0.053A before deforming, and 0.047A after deforming when the pressure is the max value of 3 MPa.

So the liquid uniform pressure can be got by measuring the quality factor Q , the equivalent impedance Z or the equivalent inductance L of the coil by the corresponding circuit.

The relationship between the output voltage of the coil and the liquid pressure loaded on the diaphragm of the sensor is

shown in Fig.5. It can be seen that the degree of linearity in the working range is good.

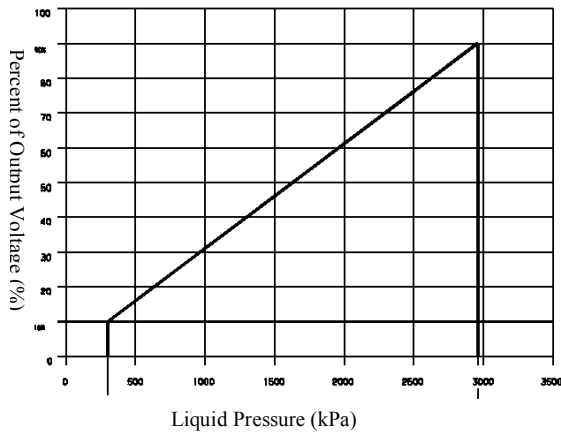


Fig.5 Relationship Between Output Voltage And Measured Liquid Pressure

VI. CONCLUSION

The magnetic flux density and the coil current density change with the deformation of the diaphragm, and the deformation is determined by the pressure loaded by the liquid, so the flux density and the current density are determined by the pressure also. And by building the appropriate circuit, the pressure can be described by the electric characters. The influence of the uniform pressure on the induced magnetic field and the eddy distribution are discussed and simulated by FEM in this paper.

ACKNOWLEDGMENT

The research work of this paper is supported by the item of technology public service platform of Jiangsu Province “Jiangsu Changzhou Service Platform of Intelligent Detection-Control and Digital Design-Manufacture Technology”, and is also supported by the item of key laboratory of Anhui Province “The Key Laboratory of Biomimetic Sensing and Advanced Robot Technology, Anhui Province”.

REFERENCES

- [1] Wang Junping, Wang An, Fan Wenxia. Study on the Effects of Coil Parameter of Electric Eddy Transducer on the Performance of Transducer [J]. Process Automation Instrumentation, 2001, 22(12): 22~24. (In Chinese)
- [2] Vyroubal D, Zele D. Experimental optimization of the probe for eddy-current displacement transducer[J]. Transactions on Instrumentation and Measurement, 1993, 42(6): 995~1000.
- [3] Cong Hua, Qiu Mianhao, etc. Computer Aided Analysis And Design of Eddy Current Sensor[J]. Journal of Test and Measurement Technology, 2000, 14(Special): 394~400. (In Chinese)
- [4] Lei Yingzhao. Analytic method of Harmonic Magnetic Field [M]. Beijing: Science Press, 2000. (In Chinese)
- [5] MARK W C. Theory for coil impedance of a conducting half space: Analytic results for eddy current analysis[J]. Journal of Applied Physics, 2001, 89(4): 2473~2481.
- [6] THEODOROS T, EPAMEINONDAS K. Series expansions in eddy current nondestructive evaluation models[J]. Journal of Material Processing Technology, 2005, 161(1~2): 343~347.
- [7] Yu Yating, Du Pingan, Wang Zhenwei. Study On the electromagnetic properties eddy current sensor[C]//Proceedings of the IEEE International Conference on Mechatronics&Automation, Niagara Falls, Canada, July, 2005: 1970~1975.
- [8] C Bartoletti, R Buommi. The design of a proximity inductive sensor [J]. Meas Sci Technol. 1998(9):1180~1190.